Phase relations and equations of state of ZrO_2 under high temperature and high pressure

O. Ohtaka, H. Fukui, T. Kunisada, and T. Fujisawa
Department of Earth and Space Science, Osaka University, Osaka 560-0043, Japan

K. Funakoshi
Japan Synchrotron Radiation Research Institute, SPring-8, Hyogo 679-5198, Japan

W. Utsumi
Japan Atomic Energy Research Institute, SPring-8, Hyogo 679-5198, Japan

T. Irifune and K. Kuroda
Department of Earth Sciences, Ehime University, Matsuyama 790-8577, Japan

T. Kikegawa
Photon Factory, KEK, Tsukuba 305-0801, Japan
(Received 26 September 2000; published 6 April 2001)

The phase relations and pressure volume dependences of ZrO_2 under high pressure and high temperature have been investigated by means of *in situ* observation using multianvil-type high-pressure devices and synchrotron radiation. By compression of 3–4 GPa, baddeleyite (monoclinic ZrO_2) transforms to two distorted fluorite (CaF_2)-type phases depending on temperature: an orthorhombic phase, orthoI, below 600 °C and a tetragonal phase above 600 °C. Both orthoI and tetragonal phases then transform into another orthorhombic phase, orthoII, with a cotunnite ($PbCl_2$)-type structure above 12.5 GPa and the phase boundary is almost independent of temperature. OrthoII is stable up to 1800 °C and 24 GPa. The unit-cell parameters and the volumes of these high-pressure phases have been determined as functions of pressure and temperature. The orthoI/tetragonal-to-orthoII transition accompanies about 9% volume decrease. The thermal expansion coefficient of orthoII at 20 GPa is $2.052\pm0.003\times10^{-5}\,K^{-1}$ over 25–1400 °C. The bulk modulus calculated using Birch-Murnaghan's equations of state is 296 GPa for orthoII, which suggests that the high-density ZrO_2 is a candidate for potentially very hard materials. The phase relation of stabilized cubic ZrO_2, CaO-ZrO_2, under pressure at elevated temperature has also been examined. Distorted fluorite-type phases do not appear in CaO-ZrO_2 but the direct transition from cubic phase to orthoII is observed on the same *P-T* conditions as in pure ZrO_2.

DOI: 10.1103/PhysRevB.63.174108 PACS number(s): 64.30.+t, 62.50.+p, 81.05.Je, 64.70.Kb

I. INTRODUCTION

Zirconia, ZrO_2, has attracted much interest since it has proven useful as refractory, as structural ceramics, as high-temperature solid electrodes, and as optical materials. Pure ZrO_2 crystallizes in the so-called baddeleyite structure (monoclinic, $P2_1/c$) under ambient conditions.[1] At high temperatures, it transforms to a tetragonal ($P4_2/nmc$),[2] and then to a cubic fluorite structure ($Fm3m$).[3] The tetragonal and cubic phases of ZrO_2 are stabilized by doping an amount of (<15 mol %) other oxides like CaO, MgO, and Y_2O_3. Since the toughening mechanism of ZrO_2 ceramics was explained by the phase transitions induced by stress field,[4,5] the high-pressure behaviors of both pure and stabilized ZrO_2 have been investigated[6–15] up to several GPa where a high-pressure phase with an orthorhombic symmetry appears. Pressure-induced phase transitions at a higher pressure range have been investigated mainly because of geophysical interest that the polymorphic structure of ZrO_2 might be a possible candidate for the high-pressure form of SiO_2.[16,17] There have been numerous contradictory results concerning the crystal structures and stability fields of ZrO_2 high-pressure polymorphs.[6,16–34] The reason for so many different results lies in the difficulties of high-pressure experiments. It is inevitable that ambiguous results appeared in early and pioneering works when experimental techniques had not been well developed. For the correct interpretation of previous studies, we note the following.

(i) When measurements are done for quenched samples, attention should be paid to whether the high-pressure and high-temperature state is really retained in the samples. Quenched samples may be a metastable phase or show some intermediate state between high- and ambient-pressure phases.

(ii) As the x-ray scattering factor of O is very small compared with that of Zr, a detailed structure determination of the O network by an x-ray method is not possible. Neutron-diffraction data, if available, are far more reliable for precise structural analysis.

(iii) There are many experimental difficulties in the *in situ* measurements under pressure. The quality of data measured under pressure is certainly worse than that obtained at ambient conditions. Such a transition as caused by a slight displacement of ions may not be detected by x-ray powder diffraction under pressure. Raman spectroscopy is a supplementary and useful tool for the identification of ZrO_2 polymorphs.

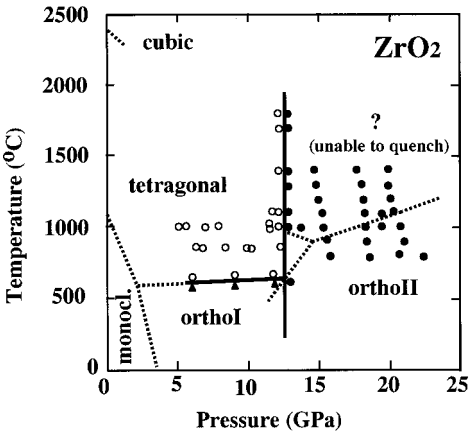

FIG. 1. Pressure-temperature phase diagram of ZrO_2. Reported boundaries are given by dashed lines: monoclinic-to-orthoI and orthoI-to-tetragonal are after Block *et al.*, (Ref. 6); monoclinic-to-tetragonal is after Witney (Ref. 18); orthoI-to-orthoII and orthoII-to-? is after Ohtaka and co-workers (Refs. 23, 27, and 29) tetragonal-to-? is assumed. Newly obtained boundaries are given by solid lines. Closed triangles, open circles, and closed circles represent orthoI, tetragonal, and orthoII, respectively.

(iv) When *in situ* observations are attempted at low temperatures, $<600\,°C$, kinetic effect and deviatoric stress should be considered. As suggested by the high melting temperature of ZrO_2, $>2680\,°C$, transitions occurring at low temperatures are very sluggish and result in a multiphase mixture over a wide range of pressure. Special attention should be paid to whether observed high-pressure phases are thermodynamically stable or not. Compression at low-temperature conditions where ionic diffusion is restrained may yield a metastable displacive-type transition. Above 10 GPa, generated pressure is not hydrostatic. Displacive-type transitions are often influenced by deviatoric stress.

(v) Results on stabilized ZrO_2 with additives may be different from those on pure ZrO_2.

On survey of the literature, we summarize the present status of high-pressure studies of ZrO_2 according to the notes mentioned above. The generalized pressure-temperature phase diagram of pure ZrO_2 is shown in Fig. 1 by dashed lines. By compression, monoclinic ZrO_2 shows a sequential transition to two orthorhombic phases (denoted as orthoI and orthoII, respectively) up to 70 GPa. As both orthoI and orthoII are quenchable to ambient conditions, precise structural analyses have been performed by neutron-diffraction studies of quenched powder samples.[12,33] OrthoI (*Pbca*) has a distorted fluorite structure similar to that of monoclinic ZrO_2 and the polyhedral coordination is 7.[12] OrthoII (*Pnam*) has a cotunnite ($PbCl_2$)-type structure and the polyhedral coordination is 9.[33] The monoclinic-to-orthoI boundary has been determined by *in situ* x-ray diffraction and Raman studies.[6,9,21] This transition is a displacive type and proceeds, though sluggish, even at room temperature.[12] The monoclinic-to-orthoI transition pressure varies largely depending upon the crystallite size in polycrystalline aggregates.[26,29] The orthoI-to-tetragonal phase boundary has been determined up to 7 GPa by *in situ* x-ray studies.[6,9] Since the orthoI-to-orthoII transition is a reconstructive type,[33] heating or excessive compression is required to promote this transition. The orthoI-to-orthoII boundary given by the dashed line in Fig. 1 was determined by synthesis experiments at elevated temperature,[23,29] while orthoII is reported to appear above 30 GPa by room-temperature compression.[30,32,34] When ZrO_2 is heated above $1000\,°C$ in the pressure range where orthoII is stable, monoclinic phase is recovered.[27] This result suggests that orthoII transforms to another unquenchable phase, denoted as? in Fig. 1, at temperatures as high as about $1000\,°C$. The boundary is indicated by a dashed line in Fig. 1. Though several structure models have been proposed for this unquenchable phase,[30,31] *in situ* studies have not been attempted so far. As shown in Fig. 1, the phase relation at elevated temperature is still unknown. Recently, both experimental and theoretical studies of the compression behavior of ZrO_2 have revealed that orthoII has a large value of bulk modulus.[30,32,34–36] As orthoII is quenchable to ambient conditions, it is a potential candidate for a new superhard material. It is therefore of great interest to obtain the reliable compression data and stability field of orthoII.

SPring-8, the third generation synchrotron radiation facility, was constructed and a bending magnet beam line equipped with a newly designed 1500-ton double-stage multianvil apparatus, SPEED-1500,[37] has become available. With this system, we are now able to perform x-ray *in situ* observations up to $2000\,°C$ over 25 GPa. High-temperature experiments enable us to study phase relations free from kinetic problems and also to collect thermal-expansion data. Even for acquiring equations of state at room temperature, preheated samples show a clear and sharp diffraction profile which results in more accurate *d*-spacing data. In this work, we attempted *in situ* observations of the ZrO_2 phases under high pressure and high temperature using the SPEED-1500 system. The main objectives are (i) to elucidate the phase relations of ZrO_2 high-pressure polymorphs at elevated temperature paying attention to their thermodynamic stabilities; (ii) to measure the compressive and thermal-expansion properties of orthoII in light of several results reported so far. We also studied the phase transitions in stabilized cubic ZrO_2, CaO-ZrO_2, under pressure because this material is often used as a part of high-pressure cell assembly and it is important to examine its stability under pressure for improving the high-pressure experimental technique.

II. EXPERIMENT

Polycrystalline pure ZrO_2 powder with nominal purity of 99.99% and CaO-ZrO_2 powder (12 mol % CaO was added) was provided by Tosoh Co. Using a multianvil apparatus, orthoI and orthoII of pure ZrO_2 were first synthesized at 6 GPa and $600\,°C$ and 20 GPa and $1000\,°C$, respectively. In order to reduce the pressure leak caused by the phase transitions, these high-pressure phases were used as starting materials for *in situ* observations, while CaO-ZrO_2 was used without any preliminary high-pressure treatments. These starting materials were pelletized and encased in sample chambers made of MgO. A mixture of ZrO_2 and Au powders (5:1 by

weight ratio) was also pelletized and put in the sample chamber separately. Because Zr ions considerably absorb x rays, the inside diameter of the sample chamber was about 800 μm.

X-ray *in situ* observations under high pressure and high temperature were performed by using properly two types of multianvil devices depending on the pressure range of interest: SPEED-1500 (Ref. 37) in SPring-8 was mainly used for experiments above 15 GPa and MAX80 (Ref. 38) in the National Laboratory for High Energy Physics for those below 15 GPa. For SPEED-1500, we used tungsten carbide cubes with truncation edge length of 3 mm as the second stage anvils. The pressure transmitting medium was sintered MgO and the gasket material was pyrophyllite. An MgO sleeve sample chamber was put between a pair of sheet heaters made of cemented TiC+diamond powders. Details of the cell assembly have been described elsewhere.[39] White x rays were directed to the sample by horizontal (0.1 mm) and vertical (0.2 mm) slits, and the diffracted beam, collimated by a 0.1-mm horizontal slit, was detected with a pure Ge solid-state detector (SSD). We used a horizontal rotating goniometer. Data collection was performed with an energy range of approximately 40–110 keV and typical duration of 300 s. MAX80 was used for single-stage compression using sintered diamond anvils with anvil top size of 3 or 4 mm. The pressure transmitting medium was a mixture of amorphous boron and epoxy resin. A pair of graphite disk furnaces and an MgO sleeve sample chamber were used. The incident white x-ray beam was collimated to 0.1 mm in height and 0.3 mm in width, and the diffracted x ray was measured with an SSD fixed on a vertically rotating goniometer. The energy range used for the analysis was approximately 40–80 keV. In both experiments of SPEED-1500 and MAX80, 2 θ angle was calibrated with the major diffraction peaks of Au at ambient condition. Temperature was monitored with a W97Re3-W74Re25 thermocouple without correction of the pressure effect on electromotive force. The fluctuation of temperature was within +0.5% throughout the present experiments up to 1800 °C. Generated pressure was determined from the unit-cell volume of Au using the equation of state.[40] At high temperatures where melting of Au occurred, pressure was estimated from the unit-cell volume of MgO using the equation of state.[41]

III. RESULTS AND DISCUSSION

A. Phase relations of pure ZrO_2

X-ray-diffraction patterns of pure ZrO_2 phases observed in the present study are shown in Fig. 2. These profiles are respective single phases and representative diffraction lines are indexed. Symbols Mg, W, and Au indicate diffractions or fluorescence of MgO sample chamber, W-Re thermocouple, and Au pressure maker, respectively. OrthoI and tetragonal phases have similar crystal structures and their x-ray-diffraction patterns resemble each other. In the present study, we have successfully distinguished them by (020), (002), and (400) diffractions of orthoI and (002) and (200) diffractions of tetragonal as shown in Fig. 2. For orthoII, 15 diffraction lines are clearly observed and used to calculate the lattice

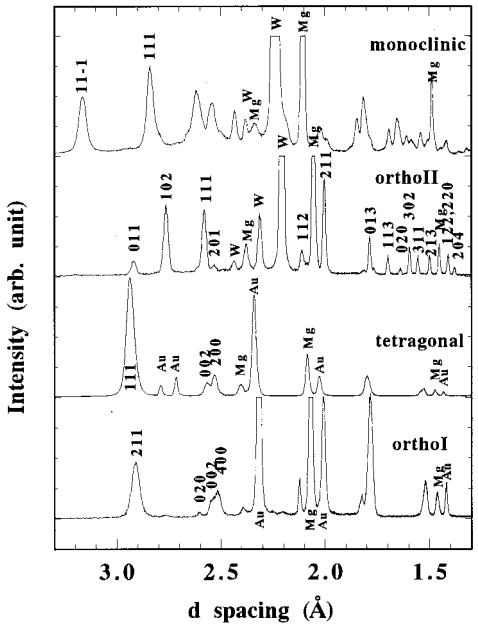

FIG. 2. Energy-dispersive x-ray-diffraction spectra of ZrO_2 phases. OrthoI is recorded at 12 GPa and 600 °C tetragonal at 6.0 GPa and 600 °C orthoII at 20 GPa and 1400 °C, and monoclinic at ambient condition recovered from 20 GPa and 1400 °C. These data were recorded at different 2θ angles and standardized by d spacing. The symbols Mg, W, and Au indicate diffractions or fluorescence of MgO sample chamber, W-Re thermocouple, and Au pressure maker, respectively.

constants. Obtained phase relations of ZrO_2 under high pressure and high temperature are shown in Fig. 1, where observed three high-pressure phases are labeled by different symbols and phase boundaries are drawn by solid lines.

In situ observations at elevated temperatures were mainly performed focusing on the stability field of orthoII. In particular, the pressure-temperature conditions where the orthoII-to-? boundary determined by synthesis experiments[27] lies were carefully examined. Combining diamond-anvil cell (DAC) and laser heating, thermally quenched ZrO_2 under pressure was found to have a hexagonal symmetry.[31] In this study, however, no phase transition was detected around 1000 °C but orthoII was observed up to 1800 °C in the pressure range from 12.5 to 22 GPa. The reported hexagonal phase is probably an artifact produced by uniaxial compression in DAC and laser heating accompanying a large thermal gradient. The quenchability of orthoII is still not well understood. In our present study, when orthoII formed at 20 GPa and 1400 °C is quenched under pressure and decompressed at room temperature, it shows a reverse transition to monoclinic phase as shown in Fig. 2. There could be a transition concerning order-disorder states that cannot be detected by the present x-ray-diffraction study. Otherwise, the quenchability may be sensitive to the experimental conditions: grain size, hydrostaticity, deviatoric stress, and decompression rate.

Above 1000 °C, the transition between tetragonal and orthoII occurs reversibly within 10 sec that are the minimum

duration needed for phase identification. Consequently, determined tetragonal-to-orthoII boundary shown in Fig. 1 is concluded to show the thermodynamic equilibrium. The boundary lies at 12.5 GPa and is almost temperature independent. The present result is slightly different from that determined by the previous synthesis experiments up to 1000 °C as indicated by the dashed line.[23,29] The difference is presumably due to the incorrect pressure estimation in the synthesis experiments. A pressure leak caused by both heating and phase transition often results in considerable deviation from conventional pressure-load calibration curves used for synthesis experiments. As apparent pressure is the more overestimated at the higher temperatures in synthesis experiments, the boundary by synthesis experiments is shifted to a higher-pressure region and has less steep slope than that by *in situ* experiments.

OrthoII is reported to appear above about 30 GPa by compression at room temperature[30,32,34] while it is synthesized around 15 GPa at high temperatures.[27] Since the orthoI-to-orthoII transition is a reconstructive type,[33] it is most plausible that the transition becomes increasingly sluggish under low temperature. In the present study, orthoI is found to transform completely into orthoII within several minutes at 600 °C. The observed transition point is 12.5 GPa and 600 °C and agrees well with that reported.[29] Though we did not examine the reversal transition this transition point is thought to be close to the thermodynamic equilibrium because the reported transition point was determined by a series of synthesis experiments for normal and reversal transitions and the pressure leak in the synthesis at 600 °C is not significant. Broad diffraction profiles of orthoI, which is shown in Fig. 2, and orthoII at 600 °C indicate that the crystal growth in large scale is inhibited and/or that shear stress exists. As the effects of kinetics and shear stress seem not to be avoided even at this temperature, we do not discuss the thermodynamic equilibrium boundary between orthoI and orthoII. The orthoI-to-orthoII boundary drawn in Fig. 1 by the solid line is the extrapolation of the tetragonal-to-orthoII boundary.

The orthoI-to-tetragonal boundary also shown in Fig. 1 is located at about 600 °C. The present result agrees fairly well with the dashed-line boundary determined by DAC experiments.[6] The almost pressure-independent phase boundary indicates that pressure has little effect on this transition. When the tetragonal phase is annealed under the stability field of orthoI, the reversal transition to orthoI does not occur. The maintained tetragonal phase shows complete transition to the monoclinic phase during decompression. As mentioned above, the broad diffraction profile of orthoI at 600 °C shown in Fig. 2 suggests the existence of shear stress. Since the orthoI-to-tetragonal transition is a displacive type that is affected by shear stress, the present orthoI-to-tetragonal boundary may not indicate the thermodynamic equilibrium, instead, it should be considered as a boundary above which the tetragonal phase is formed. Recently we determined the phase diagram of HfO_2 by means of x-ray *in situ* observations.[42] The orthoI-to-tetragonal boundary of HfO_2 is located around 1200 °C. OrthoI of ZrO_2 is less stable at the high-temperature region than that of HfO_2. By *ab initio* electronic structure calculations, Lowther *et al.*[36] showed

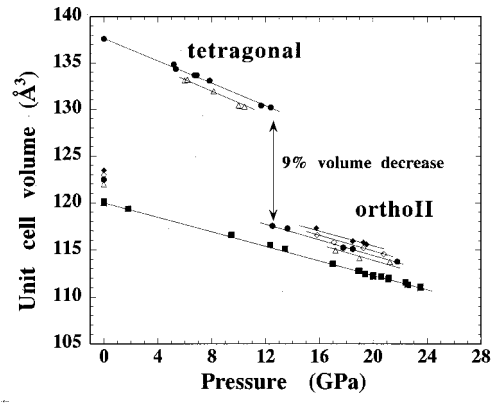

FIG. 3. Pressure dependences of the unit-cell volume (normalized as $z=4$) of orthoII and tetragonal at various temperatures. Closed squares, open triangles, closed circles, open diamonds, and closed diamonds represent room temperature, 800, 1000, 1200, and 1400 °C, respectively. The unit-cell volume of tetragonal at ambient pressure and 1000 °C is after JCPDS card no. 17-923. The unit-cell volumes of orthoII at ambient pressure and high temperatures are calculated using the thermal-expansion coefficient as described in the text.

that the fluorite-type cubic phase and orthoI of ZrO_2 are energetically more close to each other than those of HfO_2. The present result of the instability of ZrO_2 orthoI at high temperatures, in other words, the large stable field of tetragonal structure that is energetically very close to the cubic structure[15] may indirectly support the results of the calculations.

B. Static compression data for orthoII

The lattice constants of orthoII are calculated from 15 diffraction lines, while those of tetragonal are from three diffraction lines as indexed in Fig. 2. Pressure dependences of the unit-cell volume at several temperatures are shown in Fig. 3. Data collection was mainly made for orthoII over various *P-T* range and the volume changes of tetragonal at 1000 and 800 °C are added in this figure for comparison. At 1000 °C, the tetragonal-to-orthoII transition accompanies about a 9% volume decrease. Here we do not plot the data of orthoI because 600 °C above which orthoI irreversibly transforms to tetragonal is not high enough to reduce deviatoric stress and consequently nonhydrostatic effect is involved in the compression data. The unit-cell volumes of orthoII at room temperature were measured after annealing the sample above 800 °C to remove deviatoric stress.

Using the compression data shown in Fig. 3, the thermal-expansion coefficient α of orthoII is determined as follows. Since the number of data available at high temperatures is small in the narrow pressure range, the data of respective temperatures are fitted linearly and the unit-cell volumes at 20 GPa are estimated. The least-squares fit of the volumes to a linear equation as shown in Fig. 4 yields an average α at 20 GPa of $2.052\pm0.003\times10^{-5}\,K^{-1}$ over 25–1400 °C. Assuming that the pressure effect on α is negligible, unit-cell vol-

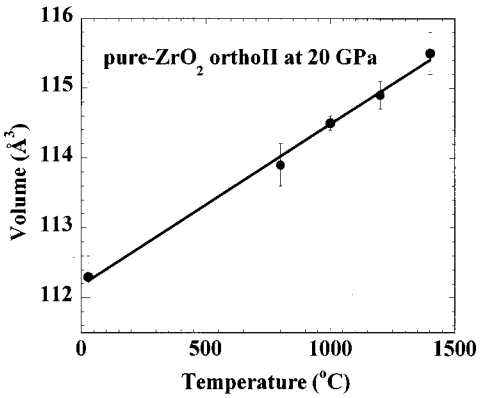

FIG. 4. Temperature-volume relation of orthoII at 20 GPa. The least-squares fit gives an average thermal-expansion coefficient of $2.052 \pm 0.003 \times 10^{-5}\ \mathrm{K}^{-1}$ over 25–1400 °C.

umes at ambient pressure V_0 under high temperatures are calculated by using thus obtained α at 20 GPa and plotted in Fig. 3. Since α should decrease with pressure from the Anderson-Gruneisen relation,[43] calculated V_0 is considered as the lowest limit of volume at each temperature. These data are fitted to the third-order Birch-Murnaghan's equations of state,[44]

$$P(V) = 1.5 \times B_0[(V/V_0)^{-7/3} - (V/V_0)^{-5/3}] \times \{1 + 0.75(B_0' - 4)[(V/V_0)^{-2/3} - 1]\}.$$

Obtained bulk moduli B_0 and their pressure derivative $B_0' = (dB/dP)_0$ at several temperatures are listed in Table I together with those previously reported. First B_0 and B_0' are refined simultaneously, which yields slightly negative values of B_0'. The values of B_0' near to 0 correspond to near-linear compression curves as shown in Fig. 3. In general, a compression curve has a near-linear part at moderate pressure range and then shows downwards-convex curvature under higher pressures. In the fitting of B_0 and B_0' to the compression curve, B_0' is most sensitive to the curvature: the larger curvature gives the larger values of B_0'. Obtained near-linear compression curves of orthoII indicate that the pressure range of present experiments is still moderate for orthoII and not high enough to determine the B_0' precisely. It is not physically reasonable to determine B_0' only from the data at the early stage of compression. Accordingly, B_0 are refined with fixed B_0' at 4 and 1. We choose these two values since $B_0' = 4$ is a usual value for many other solids[45] and $B_0' = 1$ was used for orthoII in previous study.[34] As expected from the shape of the compression curves, the data are better fitted with $B_0' = 1$ than $B_0' = 4$. Furthermore, $B_0' = 1$ gives a bulk modulus which agrees well with those determined by various methods as shown in Table I. Figure 5 shows the temperature dependences of B_0 calculated by assuming $B_0' = 1$ and 4, respectively. $B_0' = 1$ gives larger bulk modulus than $B_0' = 4$ at each temperature. The linear interpolation indicates that the temperature derivative of bulk modulus has a small negative value very close to 0. This negative temperature dependence of bulk modulus is physically reasonable. It should be noted that slightly negative values of B_0' or even $B_0' = 1$ are far from the usual values for most of the other solids, that is, 4–5.[45] Hofmeister[46] showed that values of B_0' outside the

TABLE I. Parameters of the Birch-Murnaghan equations of state of orthoII and tetragonal at several temperatures. DAC is diamond-anvil cell; EDX is energy-dispersive x-ray diffraction; ADX is angular-dispersive x-ray diffraction.

Phase	T (°C)	B_0 (GPa)	B_0'	Technique	Pressure range	Reference
OrthoII	25	265(10)	4 (fixed)	multianvil+EDX	(0–24 GPa)	This study
OrthoII	25	296(5)	1 (fixed)	multianvil+EDX	(0–24 GPa)	This study
OrthoII	800	257(20)	4 (fixed)	multianvil+EDX	(0–24 GPa)	This study
OrthoII	800	286(15)	1 (fixed)	multianvil+EDX	(0–24 GPa)	This study
OrthoII	1000	265(15)	4 (fixed)	multianvil+EDX	(0–24 GPa)	This study
OrthoII	1000	293(10)	1 (fixed)	multianvil+EDX	(0–24 GPa)	This study
OrthoII	1200	258(20)	4 (fixed)	multianvil+EDX	(0–24 GPa)	This study
OrthoII	1200	286(15)	1 (fixed)	multianvil+EDX	(0–24 GPa)	This study
OrthoII	1400	265(20)	4 (fixed)	multianvil+EDX	(0–24 GPa)	This study
OrthoII	1400	293(15)	1 (fixed)	multianvil+EDX	(0–24 GPa)	This study
OrthoII	25	332(8)	2.3	DAC+ADX	(0–50 GPa)	Haines *et al.* (Ref. 32)
OrthoII	25	306(10)	3.66 (fixed)	DAC+ADX	(0–50 GPa)	Haines *et al.* (Ref. 32)
OrthoII	25	444(15)	1 (fixed)	DAC+EDX	(0–70 GPa)	Desgreniers and Lagarec (Ref. 34)
OrthoII		305	4.68	*ab initio* calculations		Lowther *et al.* (Ref. 36)
OrthoII		314	366	*ab initio* calculations		Cohen *et al.* (Ref. 24)
OrthoII		254		Lattice-dynamic calculations		Mirgorodsky and Quintard (Ref. 35)
Tetragonal	1000	205(10)	4.0 (fixed)	multianvil+EDX	(0–12.5 GPa)	This study
Tetragonal		200	6.25	*ab initio* calculations		Dewhurst and Lowther (Ref. 14)

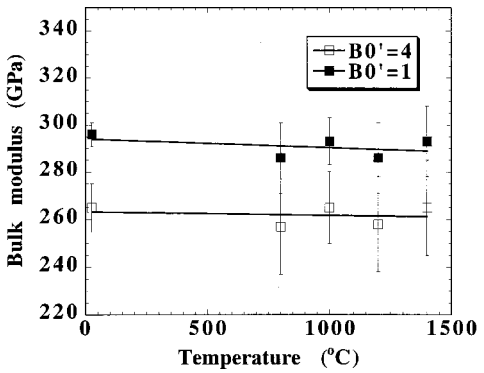

FIG. 5. Temperature dependences of bulk modulus B_0. Two sets of B_0 are calculated by assuming $B_0'=4$ and 1, respectively. Solid linear lines are given by the least-squares fit of respective data sets.

range of 3.8–8.0 lead to physically unrealistic potentials and hence are not appropriate for the Birch-Murnaghan's equations of state. On the other hand, the unusual pressure dependence of volume, namely, the near-linear compression curve of orthoII has been obtained by several experimental studies[25,34,47] as well as by the present results in which high-temperature data are included. For further understanding of the compression behavior of orthoII, experiments on extended pressure range will be necessary. The bulk modulus for tetragonal ZrO_2 at 1000 °C is added in Table I. Fitting to the Birch-Murnaghan's equations of state is successfully made with $B_0'=4$ and yields 205 GPa that shows good agreement with 200 GPa determined by *ab initio* calculations.[14]

As listed in Table I, the bulk moduli for orthoII have been reported by different methods: 444 GPa by energy-dispersive x-ray diffraction (EDX) using DAC,[34] 332 and 306 GPa by angular-dispersive x-ray diffraction (ADX) using DAC,[32] 314 and 305 GPa by *ab initio* calculations,[24,36] and 254 GPa by lattice-dynamical calculations.[35] One can notice that these DAC experiments made at room temperature have a tendency to give larger bulk moduli. Fei[48] carefully examined the effects of nonhydrostatic stress in DAC. He found that for a sample of MgO the bulk modulus determined under nonhydrostatic stress is about 15% larger than that determined under hydrostatic stress. Weidner *et al.*[49] reported that the deviatoric stress quickly approaches zero upon heating the sample above 600–800 °C. Accordingly, in DAC experiments at room temperature, special attention should be paid to deviatoric stress which makes apparent pressures high and consequently gives a large value of bulk modulus. Present bulk modulus of orthoII, 296 GPa($B_0'=1$), is discernibly higher than 254 GPa of corundum, Al_2O_3.[50] If the correlation between hardness and high bulk modulus in material is accepted,[51] orthoII of ZrO_2 is considered as a candidate for potentially ultrahard materials.

C. Cubic-orthoII transition in CaO-ZrO_2

CaO-ZrO_2 was first compressed to 10 GPa at room temperature, and then the temperature was gradually increased to 1000 °C with observing the x-ray-diffraction profile at every 100 °C. During this procedure, no phase transitions were observed. Stabilized tetragonal ZrO_2 is reported not to transform to orthoI because the difference in density is very small.[10,52] By the same manner, CaO-ZrO_2 is thought not to transform into either tetragonal or orthoI. With keeping the sample temperature at 1000 °C, pressure was increased. As shown in Fig. 6, CaO-ZrO_2 completely transforms into orthoII at 12.55 GPa which value is the same as the transition pressure for pure ZrO_2. Combining DAC and laser heating, Devi *et al.*[53] showed that CaO-ZrO_2 transforms to orthoII above 15 GPa by heating the sample above 1000 °C and that orthoII is stable up to 35 GPa. The present result is harmonious with theirs. This transition accompanies about 9% of volume decrease. CaO-ZrO_2 is often used as a part of high-pressure cell assembly in multianvil experiments because of its chemical stability and good thermal insulation. When this material is used above 12.5 GPa and elevated temperature, special attention should be paid: the cubic-to-orthoII transition causes an abrupt pressure leak and with a certain probability, the experiment will end in blowout.

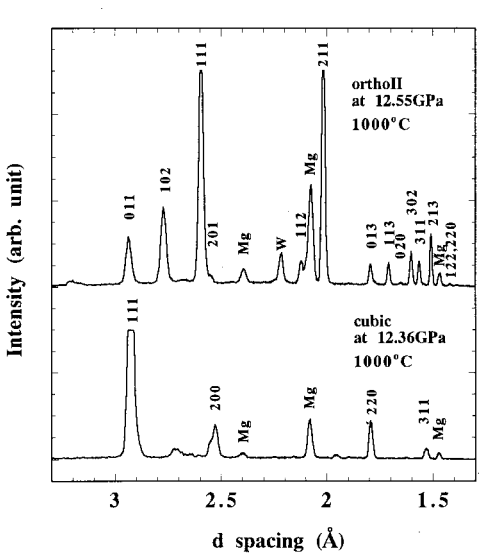

FIG. 6. Energy-dispersive x-ray-diffraction spectra of cubic and orthoII of CaO-ZrO_2. The symbols Mg and W indicate diffractions from MgO sample chamber and W-Re thermocouple, respectively.

IV. CONCLUSION

The phase relations and compression behaviors of ZrO_2 under high pressure and high temperature have been investigated by means of *in situ* observations using multianvil high-pressure devices and synchrotron radiation. Stability fields of orthoI, tetragonal, and orthoII have been determined. OrthoI is stable from 4 to 12.5 GPa below 600 °C and transforms to the tetragonal phase above this temperature. The almost pressure-independent phase boundary between orthoI and tetragonal indicates that pressure has little effect on this transition. Both orthoI and tetragonal transform to orthoII above 12.5 GPa accompanying about 9% volume decrease and the phase boundary is almost independent of temperature. OrthoII is stable up to 1800 °C and 24 GPa. The unit-cell parameters and the volumes of orthoII and tetragonal have

been determined as functions of pressure and temperature. The thermal-expansion coefficient of orthoII at 20 GPa is $2.052 \pm 0.003 \times 10^{-5}\ K^{-1}$ over 25–1400 °C. The bulk moduli of orthoII calculated using Birch-Murnaghan's equation of state is 296 GPa. The present result indicates that orthoII is highly incompressible and thus a candidate for ultrahard materials. Neither orthoI nor tetragonal appears in CaO-ZrO_2 but the direct transition from cubic to orthoII is observed on the same P-T conditions as in pure ZrO_2.

ACKNOWLEDGMENTS

O.O. is grateful to T. Kotani for helpful discussion. This research was performed under the approval of the Japan Synchrotron Radiation Research Institute (JASRI) (Proposal No. 1998A0187-CD-np and 1999A0004-CD-np) and that of the Photon Factory Advisory Committee (Proposal No. 97G243).

[1] C. J. Howard, R. J. Hill, and B. E. Reichert, Acta Crystallogr., Sect. B: Struct. Sci. **44**, 116 (1988).
[2] G. Teufer, Acta Crystallogr. **15**, 1187 (1962).
[3] R. W. G. Wyckoff, *Crystal Structures*, 2nd ed. (Wiley, New York, 1963), Vol. 1.
[4] T. K. Gupta, F. F. Lange, and J. H. Bechtold, J. Mater. Sci. **13**, 1464 (1978).
[5] W. M. Kriven, J. Am. Ceram. Soc. **71**, 1021 (1988).
[6] S. Block, J. A. H. da Jornada, and G. J. Piermarini, J. Am. Ceram. Soc. **68**, 497 (1985).
[7] R. Suyama, T. Ashida, and S. Kume, J. Am. Ceram. Soc. **68**, c-134 (1985).
[8] R. Suyama, H. Takubo, and S. Kume, J. Am. Ceram. Soc. **68**, c-237 (1985).
[9] H. Arashi, O. Shimomura, T. Yagi, S. Akimoto, and Y. Kudoh, Adv. Ceram. **24**, 493 (1988).
[10] O. Ohtaka, T. Iwami, K. Urabe, and S. Kume, J. Am. Ceram. Soc. **71**, c-164 (1988).
[11] A. H. Heuer, V. Lanteri, S. C. Farmer, R. Chaim, R. R. Lee, B. W. Kibbel, and R. M. Dickerson, J. Mater. Sci. **24**, 124 (1989).
[12] O. Ohtaka, T. Yamanaka, S. Kume, N. Hara, H. Asano, and F. Izumi, Proc. Jpn. Acad., Ser. B: Phys. Biol. Sci. **66**, 193 (1990).
[13] C. J. Howard, E. H. Kisi, and O. Ohtaka, J. Am. Ceram. Soc. **74**, 2321 (1991).
[14] J. K. Dewhurst and J. E. Lowther, Phys. Rev. B **57**, 741 (1998).
[15] G. Jomard, T. Petit, A. Pasturel, L. Magaud, G. Kresse, and J. Hafner, Phys. Rev. B **59**, 4044 (1999).
[16] L. G. Liu, J. Phys. Chem. Solids **41**, 331 (1980).
[17] L. G. Liu and W. A. Basset, in *Elements, Oxides, and Silicates: High-Pressure Phases with Implications for the Earth's Interior* (Oxford University Press, New York/Oxford, 1986), p. 250.
[18] E. D. Witney, J. Electrochem. Soc. **112**, 91 (1965).
[19] G. L. Kulcinski, J. Am. Ceram. Soc. **51**, 582 (1968).
[20] G. Bocquillon and C. Susse, Rev. Int. Hautes Temp. Refract. **6**, 263 (1969).
[21] H. Arashi and M. Ishigame, Phys. Status Solidi A **71**, 313 (1982).
[22] Y. Kudoh, H. Takeda, and H. Arashi, Phys. Chem. Miner. **13**, 233 (1986).
[23] O. Ohtaka, E. Ito, and S. Kume, J. Am. Ceram. Soc. **71**, c-448 (1988).
[24] R. E. Cohen, M. J. Mehl, and L. L. Boyer, Physica B **150**, 1 (1988).
[25] H. Arashi, T. Yagi, S. Akimoto, and Y. Kudoh, Phys. Rev. B **41**, 4309 (1990).
[26] S. Kawasaki, T. Yamanaka, S. Kume, and T. Ashida, Solid State Commun. **76**, 527 (1990).
[27] O. Ohtaka, E. Ito, and S. Kume, J. Am. Ceram. Soc. **73**, 744 (1990).
[28] G. A. Kourouklis and E. Liarokapis, J. Am. Ceram. Soc. **74**, 520 (1991).
[29] O. Ohtaka, T. Yamanaka, S. Kume, E. Ito, and A. Navrostky, J. Am. Ceram. Soc. **74**, 505 (1991).
[30] J. M. Leger, P. E. Tomaszewski, A. Atouf, and A. S. Pereira, Phys. Rev. B **47**, 14 075 (1993).
[31] O. Ohtaka, T. Yamanaka, and T. Yagi, Phys. Rev. B **49**, 9295 (1994).
[32] J. Haines, J. M. Leger, and A. Atouf, J. Am. Ceram. Soc. **78**, 445 (1995).
[33] J. Haines, J. M. Leger, S. Hull, J. P. Petitet, A. S. Pereira, C. A. Perottoni, and J. A. H. da Jornada, J. Am. Ceram. Soc. **80**, 1941 (1997).
[34] S. Desgreniers and K. Lagarec, Phys. Rev. B **59**, 8467 (1999).
[35] A. P. Mirgorodsky and P. E. Quintard, J. Am. Ceram. Soc. **82**, 3121 (1999).
[36] J. E. Lowther, J. K. Dewhurst, J. M. Leger, and J. Haines, Phys. Rev. B **60**, 14 485 (1999).
[37] W. Utsumi, K. Funakoshi, S. Urakawa, M. Yamakata, K. Tsuji, H. Konishi, and O. Shimomura, Rev. High Pressure Sci. Technol. **7**, 1484 (1998).
[38] O. Shimomura, Physica B & C **139 & 140B**, 292 (1986).
[39] T. Irifune, N. Nishiyama, K. Kuroda, T. Inoue, M. Isshiki, W. Utsumi, K. Funakoshi, S. Urakawa, T. Uchida, T. Katsura, and O. Ohtaka, Science **279**, 1698 (1998).
[40] O. L. Anderson, D. G. Isaak, and S. Yamamoto, J. Appl. Phys. **65**, 1534 (1989).
[41] J. C. Jamieson, J. N. Fritz, and M. H. Manghnani, in *High Pressure Research in Geophysics* (Center for Academic Publishing, Tokyo, 1982), p. 27.
[42] O. Ohtaka, H. Fukui, T. Kunisada, T. Fujisawa, K. Funakoshi, W. Utsumi, T. Irifune, K. Kuroda, and T. Kikegawa, J. Am. Ceram. Soc. (to be published).
[43] O. L. Anderson, E. Schreiber, R. C. Liebermann, and N. Soga, Rev. Geophys. **6**, 491 (1968).
[44] F. Birch, Phys. Rev. **71**, 809 (1947).
[45] J. D. Bass, in *Mineral Physics & Crystallography* (American Geophysical Union, Washington, DC, 1995), p. 45.
[46] A. M. Hofmeister, Geophys. Res. Lett. **20**, 635 (1993).
[47] L. C. Ming and M. H. Manghani, in *Solid State Physics under Pressure* (Terra Scientific, Tokyo, 1985), p. 135.
[48] Y. Fei, Am. Mineral. **84**, 272 (1999).
[49] D. J. Weidner, M. T. Vaughan, J. Ko, Y. Wang, X. Liu, A. Yeganeh-Haeri, R. E. Pacalo, and Y. Zhao, in *High Pressure*

Research: Application to Earth and Planetary Science (American Geophysical Union, Washington, DC, 1992), p. 13.
[50] I. Ohno, S. Yamamoto, and O. L. Anderson, J. Phys. Chem. Solids **47**, 1103 (1986).
[51] W. Yang, R. G. Parr, and L. Uytterhoeven, Phys. Chem. Miner. **15**, 191 (1987).
[52] H. Toraya, O. Ohtaka, and S. Kume, Mineral. J. **13**, 500 (1987).
[53] S. R. U. Devi, L. C. Ming, and M. H. Manghnani, J. Am. Ceram. Soc. **70**, c-218 (1987).